All aqueous multi-phase systems and emulsions formed via low concentrated ultra-high molar mass polyacrylamides

Alexander Plucinski,[†] Marko Pavlovic[‡] and Bernhard V. K. J. Schmidt[,†]*

[†]School of Chemistry, University of Glasgow, Glasgow G12 8QQ, UK

[‡]Department of Colloid Chemistry, Max Planck Institute of Colloids and Interfaces, Am Mühlenberg 1, 14476 Potsdam, Germany

Keywords: Aqueous multi-phase system, reversible addition fragmentation chain transfer (RAFT) polymerisation, ultra-high molecular weight (UHMW) polymers, water in water emulsion

For table of content use only

All aqueous multi-phase systems and emulsions formed via low concentrated ultra-high molar mass polyacrylamides

Alexander Plucinski,[†] Marko Pavlovic[‡] and Bernhard V. K. J. Schmidt[*,†]*

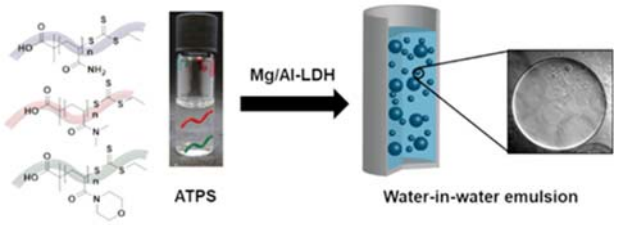

Abstract

Aqueous multi-phase systems have attracted a broad interest in recent years, which is mainly due to their applicability in biology for purification and isolation of bio molecules but also for separation of particles as well as environment for enzymatic reactions. In here, three polyacrylamides poly(*N*,*N*-dimethylacrylamide) (PDMA), poly(acrylamide) (PAAM), and poly(4-acryloylmorpholine) (PAM) with ultra-high molar mass were synthesised *via* photo induced RAFT polymerisation (M_n > 700000 g mol^{-1}). The polymers were combined to form aqueous multi-phase systems with low total polymer concentration as low as 1.1 to 2.1 wt%. Furthermore, the aqueous multi-phase system could be transformed into water-in-water (w/w) emulsions, stabilised by layered double hydroxide particles. Due to the low polymer content, these aqueous multi-phase systems open up new pathways for example in the separation of bio molecules or the compartmentalisation of aqueous environments in catalysis.

Introduction

Water-based polymer systems constitute an important area in biology,[1, 2] medicine[2] or food industry.[3] An interesting and unique property of water-based polymer systems is the aqueous two-phase system (ATPS), which forms via liquid-liquid phase separation of two compounds dissolved in water.[4] Due to the incompatibility, of these two compounds *e.g.* polymer/polymer or salt/polymer, the formation of two macroscopic aqueous phases take place.[5-8] The ability for the formation of multiple macroscopic aqueous phases are useful for various applications in areas of food industry[9] as well as extraction, purification, and separation of bio molecules,[10, 11] proteins[12] or metal ions.[13, 14] The most frequently utilised system, employing two polymers, makes use of poly(ethylene glycol) (PEG) and dextran (Dex).[12, 15] The mixture of these two polymers forms an

ATPS, with one homopolymer highly enriched in one phase and the second homopolymer highly enriched in the other phase, when the concentration exceeds the critical polymer concentration. Recently the ATPS based on PEG and Dex attracted attention for various applications *e.g.* for the formation of Janus droplets,[16, 17] protein localisation within giant vesicles[18] or enzymatic cascade reactions.[19]

In relation with ATPSs, water-in-water (w/w) emulsions caught considerable attention,[20, 21] due to the high biocompatibility of theses emulsions. The dispersion of two thermodynamic incompatible aqueous solutions of macromolecules *e.g.* hydrophilic polymers forms a w/w emulsion.[22] Different polymer mixtures were used in ATPSs for w/w emulsion formation *e.g.* PEG and Dex,[23] Dex and methylcellulose[24] or gelatin and Dex.[25] Similar to ATPS, the polymer combination PEG and Dex is most frequently utilized for the formation of w/w emulsions. Common, emulsions like water-in-oil (w/o) or oil-in-water (o/w) emulsions can be stabilised by surfactants or larger particles.[26] In contrast, emulsion stabilisation based on surfactants is not suitable for w/w emulsions because of the significant lower interfacial tension of the ATPS and a very broad interface between the aqueous phases at which small surfactant molecules cannot align properly.[27, 28] Therefore, particles have to be employed to form w/w Pickering emulsions. In the case of PEG and Dex ATPS, various types of particles were introduced to stabilise the w/w emulsion *e.g.* cellulose nanocrystals,[29] polydopamine particles[30, 31] or thermoresponsive double hydrophilic block copolymers.[32] Peddireddy *et al.* described that due to the high anisotropy in the form of nanorods, cellulose nanocrystals can stabilise w/w emulsions effectively.[29] Moreover, platelets like layered double hydroxide (LDH) nanoparticles[33, 34] are another avenue to stabilise w/w emulsions,[35] hydrogels[33] or suspensions.[34] For example, Inam *et al.* showed that 2D diamond-shape poly(lactide) block copolymer nanoplatelets can successfully stabilise w/w emulsions. Due

to the considerable surface and significant interface to volume ratio, especially larger platelets exhibit strong emulsion stabilisation effect.[35]

Besides ATPS, aqueous multiphase systems featuring more than two phases are under investigation as well.[17, 36-39] Akbulut *et al.* conducted the formation of a plethora of aqueous multiphase systems based on different hydrophilic polymers[36] and employed them for separation of nanoparticles with different size and shape.[37] Furthermore, Beldengrün *et al.* investigated a multiple water-in-water-in-water (w/w/w) emulsion using a maltodextrin/gelatin/maltodextrin system.[40] In the literature a significant number of studies were presented regarding the influence of molar mass on the formation of ATPS.[41-44] These studies showed that the location of the binodal, which is the line that separates one- and two-phase region of the phase diagram, strongly depends on the molar mass of the used polymers. In the example for the system PEG and Dex, the higher the molar mass, the lower the required concentration for ATPS formation.[41, 42] However, most frequently ATPS are formed with a polymer concentration above 4 wt%. In order to decrease the required amount of polymer material for a stable ATPS, increased molar mass of the employed polymers could be a useful development for the field. In addition, the investigation of new combinations of polymers for ATPS formation might reveal additional features regarding the phase separation behaviour. Especially, synthetic hydrophilic polymers enable a tailored design of the polymer components, e.g. regarding molar mass or polymer architecture.

Due to their aggregation behaviour in water as part of double hydrophilic block copolymers, poly(acrylamides) represent a good choice for an ATPS and the formation of w/w emulsions.[45-47] To investigate novel high molar mass poly(acrylamide) based ATPS, reversible-deactivation radical polymerisation like reversible addition fragmentation chain transfer (RAFT) polymerisation, is a good approach to synthesise poly(acrylamides).[48-53] Especially the procedure

from Sumerlin and co-workers seems promising to obtain high molar mass poly(acrylamides) as performed *via* photo induced (PI) RAFT polymerisation,[50] which readily achieves molar masses above $1 \cdot 10^6$ g·mol^{-1}.

Herein, the phase behaviour of three different high molar mass hydrophilic polymers in ATPS formation is investigated. Therefore three polymers with high molar mass, i.e. poly(*N*,*N*-dimethylacrylamide) (PDMA), poly(acrylamide) (PAAM), and poly(4-acryloylmorpholine) (PAM), were synthesized *via* PI-RAFT polymerisation. Subsequently, the polymers were analysed by ^{1}H-NMR spectroscopy and size exclusion chromatography (SEC). Additionally, the mixtures of each polymer combination, at low concentrations, were investigated revealing the formation of ATPS or aqueous three phase system (A3PS). Moreover, the ATPSs were used to form w/w emulsions, stabilised with Mg/Al-CO_3-LDH nanoparticles. These emulsions were further analysed *via* confocal laser scanning microscopy (CLSM). In order to localise the polymer in the emulsion, Rhodamine B (RhB), fluorescein and Coumarin labelled hydrophilic polymers were employed. Unprecedented aggregative phase behaviour of the different poly(acrylamides) was observed in w/w emulsions opening up new opportunities for the design of aqueous multi-phase systems.

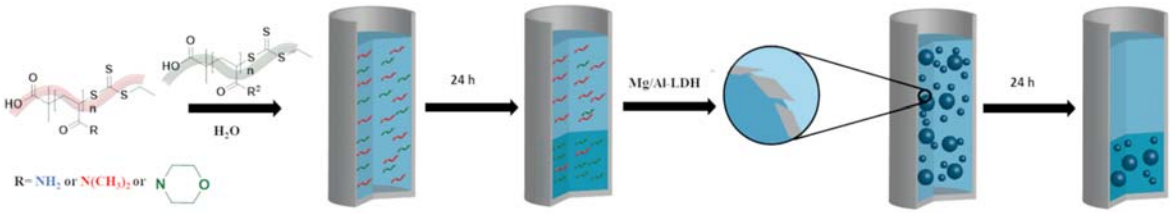

Scheme 1. ATPS formation on the example of poly(*N*,*N*-dimethylacrylamide) (PDMA) (red) and poly(4-acryloylmorpholine) (PAM) (green) as well as water-in-water emulsion stabilised by Mg/Al-CO_3- layered double hydroxide (LDH) nanoparticles (grey).

Experimental Part

Materials

Acetone (Fisher, analytical grade), acetic acid (1.0 N, VWR) 4-acryloylmorpholine (AM, 98%, Sigma-Aldrich, passed over a column of basic aluminium oxide), acrylamide (AAM, 98%, Sigma-Aldrich), aluminium nitrate nonahydrate (98%, Sigma-Aldrich), 2-bromisobutyric acid (98.5%, pure, Sigma Aldrich), carbon disulfide (CS_2, 99%, Sigma-Aldrich), dimethyl sulfoxide (DMSO; Merckmillipore, Emsure®, ACS), *N,N*-dimethylacrylamide (DMA, 99%, Sigma-Aldrich, passed over a column of basic aluminium oxide), ethanethiol (98%, Alfa Aesar), ethyl acetate (99.5%, VWR), Fluorescein isothiocyanate (FITC, Sigma-Aldrich), n-hexane (95%, Sigma-Aldrich), hydrochloric acid (conc., Fisher), *N*-methyl-2-pyrrolidone (NMP, Fluka, GC grade), magnesium nitrate hexahydrate (99.9%, Sigma-Aldrich), Millipore water (obtained from a Sartorius arium pro ultrapure water system), potassium phosphate (K_3PO_4, Sigma Aldrich), Rhodamine B isothiocyanate (RITC, Sigma-Aldrich) sodium acetate (anhydrous, 98 %, Fisher), tetrahydrofuran (THF, extra dry, Acros Organics) and 7-[4-(trifluoromethyl)coumarin]acrylamide (98%, Sigma-Aldrich) were used as received unless otherwise noted. 2-(((Ethylthio)carbonothioyl)thio)-2-methylpropanoic acid (EMP)[54, 55] and LDH[56-58] were synthesised according to the literature.

For the photo-induced RAFT (PI-RAFT) polymerisation, UV-light (UV nail-light-setting-lamp, λ = 365 nm) was employed.

PI-RAFT-polymerisation of DMA

Destabilised DMA (1.0 g, 10 mmol, 15151 eq.), EMP (146 µL, 0.06 µmol, 1.0 eq. from a DMSO stock 1 mg mL^{-1} DMSO), and acetate buffer (1 mL, 0.2 M, pH=5) were mixed in a vial (7 mL) containing a stirring bar and sealed with a septum. The solution was bubbled for 30 min with nitrogen and the polymerisation was initiated by an UV-lamp (nail-lamp). The polymerisation was stopped after 24 h. Subsequently, the polymer was dialysed against deionised water (Spectra/Por 3500 Da) for 3 days. Finally, the sample was freeze-dried and a white solid (780 mg, M_n= 1.07 · 10^6 g · mol^{-1}) was obtained.

PI-RAFT-polymerisation of acrylamide

In a glass vial (7 mL) AAM (1.0 g, 14 mmol, 21000 eq.) was dissolved under stirring in acetate buffer (1 mL, 0.2 M, pH=5). Subsequently, EMP (146 µL, 0.06 µmol, 1.0 eq. from a DMSO stock 1 mg mL^{-1} DMSO) was added and the vial (7 mL) containing a stirring bar was sealed with a septum. The solution was bubbled for 30 min with nitrogen and the polymerisation was initiated by an UV-lamp (nail-lamp). The polymerisation was stopped after 24 h. Subsequently, the polymer was dialysed against deionised water (Spectra/Por 3500 Da) for 3 days. Finally, the sample was freeze-dried and a white solid (995 mg, M_n= 730000 g · mol^{-1}) was obtained.

PI-RAFT-polymerisation of 4-acryloylmorpholine

Destabilised AM (1.0 g, 7.0 mmol, 10640 eq.), EMP (146 µL, 0.06 µmol, 1.0 eq. from a DMSO stock 1 mg mL^{-1} DMSO), and acetate buffer (1 mL, 0.2 M, pH=5) were mixed in a vial (7 mL) containing a stirring bar and sealed with a septum. The solution was bubbled for 30 min with nitrogen and the polymerisation was initiated by an UV-lamp (nail-lamp). The polymerisation was

stopped after 24 h. Subsequently, the polymer was dialysed against deionised water (Spectra/Por 3500 Da) for X days. Finally, the sample was freeze-dried and a white solid (990 mg, M_n= 1.04· 10^6 g · mol^{-1}) was obtained.

Preparation of ATPS and phase diagram

Dried PDMA (25 mg) was dissolved in deionised water (475 mg), to obtain a 5 wt% solution. A 5 wt% solution of PAAM was prepared in the same way. Afterwards both solutions were mixed to receive a 2.5 wt% / 2.5 wt% mixture. Subsequently, the solution was equilibrated at ambient temperature in order to demix, investigated and diluted (100 mg of deionised water each cycle). The process was repeated, until no phase separation was observed, which was recorded as the data point of the binodal curve. All other concentration combinations were conducted in a similar way.

Preparation of A3PS and phase diagram

Dried PDMA (20 mg), PAAM (20 mg), and PAM (20 mg) were dissolved in deionised water (940 mg) to obtain a 2 wt% / 2 wt% / 2 wt% mixture. Subsequently, the solution was mixed, equilibrated at ambient temperature in order to demix, investigated and diluted (100 mg of deionised water each cycle). The process was repeated, until no phase separation was observed, which was recorded as the data point of the binodal curve. All other concentration combinations were conducted in a similar way.

Preparation of w/w emulsions

Dried PDMA (30 mg) and PAAM (30 mg) were dissolved in water (940 mg) to form a 3.0/3.0 wt% solution. LDH particles (2.0 mg) were dispersed in water (998 mg) to generate a 0.2 wt%

dispersion. Both solutions were combined to obtain 1.5/1.5 wt% polymer and 0.1 wt% LDH particles in the mixture. The mixture was subjected to ultrasonic treatment for two minutes as well as shaking by hand for one minute and subsequently analysed *via* CLSM. The sample was again analysed *via* CLSM after 24 h and phase separation observed. All other concentration combinations were conducted in a similar way.

Preparation of w/w emulsions with additional labelled polyacrylamides

Dried PDMA (12 mg), RITC-PDMA (3 mg), PAM (12 mg) and FITC-PAM (3 mg) were dissolved in water (470 mg) to form a 3.0/3.0 wt% solution. LDH particles (1.0 mg) were dispersed in water (499 mg) to generate a 0.2 wt% dispersion. Both mixtures were combined to obtain 1.5/1.5 wt% polymer and 0.1 wt% LDH particles in the mixture. The mixture was subjected to ultrasonic treatment for two minutes as well as shaking by hand for one minute and subsequently analysed via CLSM. The sample was again analysed *via* CLSM after 24 h and phase separation observed. All other combinations were conducted in a similar way.

Analytical methods

^{1}H-NMR spectra were recorded in deuterium oxide (D_2O, Aldrich) at ambient temperature at 400 MHz with a Bruker Ascend400. Size exclusion chromatography (SEC) of PDMA and PAAM were conducted in 0.1 M aqueous $NaNO_3$ buffer at 25 °C using a column system with a PL Aquagel-OH Guard and PL Aquagel-OH MIXED-H and Viscotek VE 3580 RI detector and Viscotek SEC-MALS 20 for the molar mass determination. The system was calibrated with pullulan standards. SEC of PAM was conducted in THF at 25 °C using a PSS SD guard column,

a PSS SDV-Linear-M column, Wyatt Optilab DSP RI detector and a Wyatt DAWN EOS detector. A Brookhaven differential refractometer was used for the determination of d*n*/d*c* (Table S1).

Confocal laser scanning microscopy (CLSM) and bright field microscopy were performed on Zeiss LSM710 confocal microscope (Zeiss, Göttingen, Germany) and software Carl Zeiss ZEN 2011 v7.0.3.286. LD EC Epiplan NEUFLUAR 50X, 0.55 DIC (Carl Zeiss, White Plains, NY, USA), NEUFLUAR 20X, 0.55 DIC (Carl Zeiss, White Plains, NY, USA) and N-Achroplan 10x/0.25 Ph 1 (Carl Zeiss, White Plains, NY, USA) objectives were used. All samples were prepared in a CELLview (Greiner Bio-One, Stonehouse, UK) 35 mm plastic cell culture dish with a borosilicate glass bottom. The images were taken with three different channels, two for the particular dyes (RITC, FITC or coumarin) and one for a bright field image. Dynamic light scattering (DLS) was performed on a ZetaSizer by Malvern with water as solvent. The size of the emulsion droplets was determined over 30 particles from bright field images and averaged. The error is based on the standard deviation. The partition coefficients were determined via the concentration calculated from the NMR using DMF as internal standard according to equation S1 for the ATPS and equation S2 for the A3PS.

Results and Discussion

Synthesis of Polyacrylamides via photo induced RAFT polymerisation

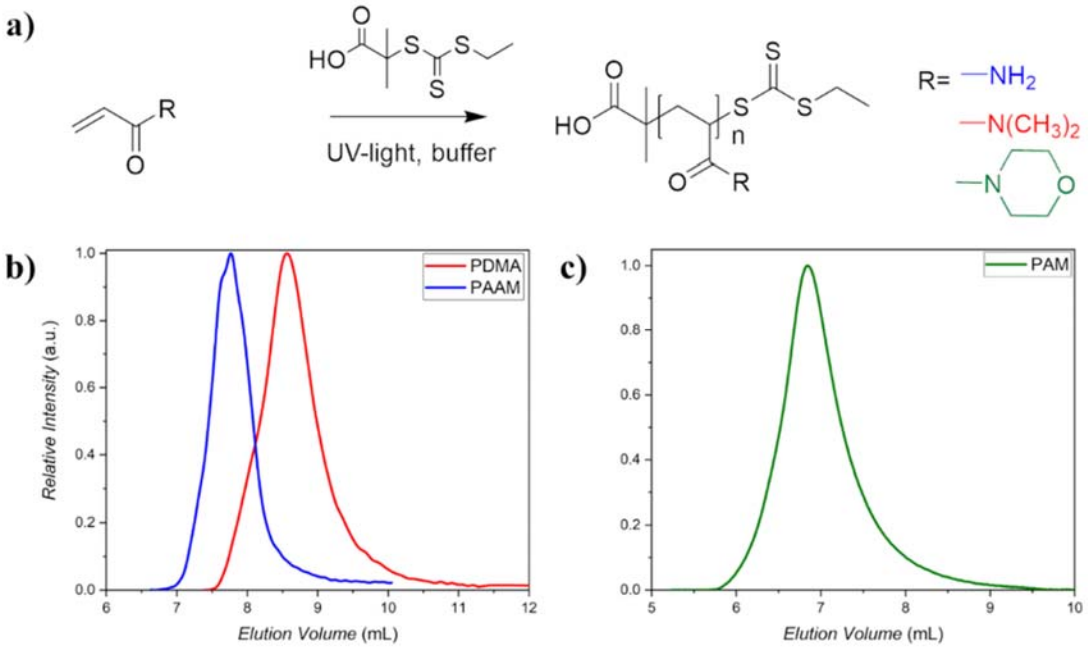

Figure 1. (a) Reaction scheme of the PI RAFT-polymerisation of acrylamides with EMP as chain transfer agent, (b) SEC chromatogram of PDMA and PAAM measured in 0.1 N $NaNO_3$ buffer, (c) SEC chromatogram measurement of PAM measured in THF.

RAFT polymerisation is a well-known an avenue to synthesise polymers like poly(*N*,*N*-dimethylacrylamide) (PDMA), poly(acrylamide) (PAAM) and poly(4-acryloylmorpholine) (PAM). In order to synthesise high molar mass poly(acrylamides) the procedure of Sumerlin and coworkers was employed.[50] EMP was used as chain transfer agent and the reaction was initiated in acetate buffer *via* UV-light (nail-lamp, λ=365 nm). A high concentrated solution of monomer (> 7 M) was utilised and the ratio between monomer and EMP was adjusted to 10000-21000

(depending on the monomer): 1 to obtain a theoretical molar mass of around $1.5 \cdot 10^6$ g·mol^{-1}. To obtain a high molar mass a low amount of EMP was employed, and the reaction was initiated by UV-light, to decrease the number of radicals in the reaction and enable fast initiation, in comparison to the thermal RAFT-polymerisation with exogenous radical initiation. All conversions were determined by ^{1}H-NMR (**Figure S2-S4**), which revealed a quantitative monomer conversion for AAM as well as AM and 70% for DMA. The poly(acrylamide) products were analysed *via* SEC-MALS revealing ultra-high molar masses and rather broad molar mass distributions with M_n= 1.07 · 10^6 g · mol^{-1} and $Đ$ = 1.4 for PDMA, M_n= 730000 g · mol^{-1} and $Đ$ = 1.7 for PAAM, and M_n= 1.04· 10^6 g · mol^{-1} and $Đ$ = 1.5 for PAM (**Figure 1** and **Table S1**). Although RAFT polymerisation was employed, rather high $Đ$ were observed which might be due to a low efficiency of initiation, *i.e.* radical termination and low initiation rate, as also obvious by the tailing of the polymer related peaks in SEC towards lower molar masses. In addition, the degradation of the RAFT end groups could be caused by UV irradiation with too high intensity.

ATPS of ultra-high molar mass acrylamides

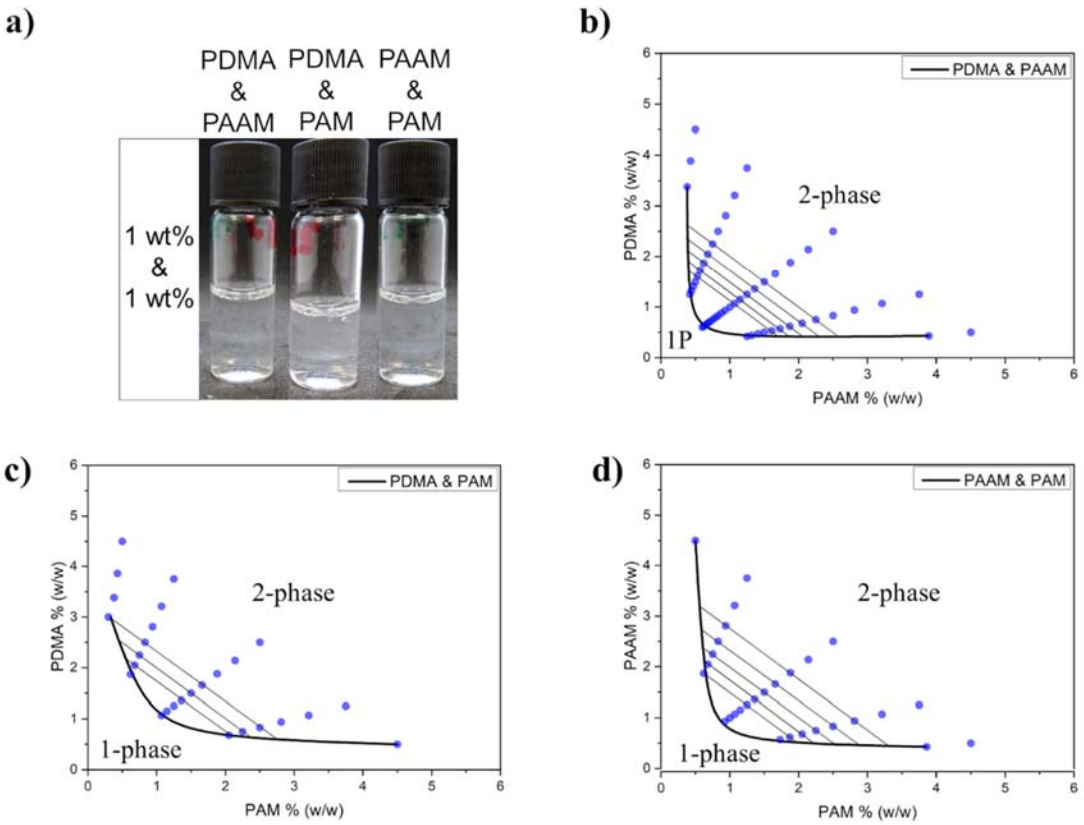

Figure 2. (a) ATPS of each combination at a total polymer concentration of 2 wt% (1 wt%/1 wt%). (b-d) Phase diagrams of the ATPS for all polymer combinations showing the experimental binodals (black curves), the dilution steps (blue dots) and tie-lines: (b) PDMA and PAAM, (c) PDMA and PAM, (d) PAAM and PAM.

In order to elucidate the phase behaviour of the different ultra-high molar mass poly(acrylamide) mixtures in aqueous solution, ATPS formation of the three poly(acrylamides) were investigated. For that, a phase diagram was assembled for each combination (PDMA/PAAM, PDAM/PAM, and PAAM/PAM). To analyse the phase behaviour of the ATPSs, five differently concentrated stock

solutions were prepared for all combinations (9, 7.5, 5, 2.5, and 1 (wt/wt)). Two different stock solutions were mixed together to obtain a total polymer concentration of 5 wt% (4.5/0.5, 3.75/1.25, 2.5/2.5, 1.25/3.75 and 0.5/4.5 (wt/wt)). Subsequently, the solutions were mixed, equilibrated at ambient temperature to demix, investigated, and diluted to find the concentration at which only one phase is observed (**Figure 2a**). To generate the phase diagram, the last concentration, where a phase separation was observed was used as data point in the binodal, which is the line that separates one- and two-phases in the graph.

The binodal was located at significantly lower concentrations, for the combination of PDMA and PAAM, in comparison to the ATPS of Dex/PEG (**Figure 2b**). The lowest concentration for an observed ATPS, for the equal concentration of the polymers, was 0.56 wt%. For the ATPS formed by PDMA and PAM (**Figure 2c)**, the slope of the binodal was more flat than for PDMA/PAAM. The lowest concentration for an observed ATPS, for the equal concentration of the polymers, was 0.9 wt%. The phase diagram for the combination of PAAM and PAM (**Figure 2d)** is similar to the phase diagrams of the previous combinations. The minimal concentration for a stable ATPS was found to be at 0.79 wt%. Surprisingly the results show that the mixtures of the most hydrophilic polymers (PDMA & PAAM) require the lowest concentration for phase separation. This in contrast to our expectation that for the formation of a macroscopic phase separation, the combination featuring the most different hydrophilicity should form the most stable phase separation. One reason for that could be the influence of the high hydration enthalpies of PDMA and PAAM, which equalise the loss of entropy during the phase separation. In order to understand these differences, the location of each polymer was detected *via* ^{1}H-NMR of each phase (**Figure S5-S8**, **Table S2**) with DMF as internal standard. The results showed for the combination of PDMA and PAAM, after 24 hours, a clear separation of the polymers in the phases (**Figure S5**

and **S8a**). PDMA was located in the upper and PAAM in the lower phase with partition coefficients of 100 for PDMA and 0.01 for PAAM, which is similar to the most studied ATPS formed by PEG and Dex.[14] In here, the PEG is enriched in the upper phase and Dex is enriched in the lower phase. The combination of PDMA and PAM showed a less clear separation after 24 hours with partition coefficients of 2.91 for PDMA 0.13 for PAM. PAM was located in the lower phase but PDMA is present in both phases (**Figure S6** and **S8b**). In the case of PAAM and PAM, the polymers are clearly separated in different phases. However, in both phases, a small amount of the other polymer is present and partition coefficients of 2.4 for PAAM and 0.06 for PAM were observed (**Figure S7** and **S8c**). The NMR results show that the combination with the best separation of the polymers also features the lowest concentration required for phase separation (PDMA and PAAM). One reason for the good phase separation of PDMA and PAAM could be the high hydrophilicity of both polymers and thereby significant water polymer interaction. Apparently, the extent of separation of the polymers in different phases is an important parameter to lower the concentration required for ATPS formation. Furthermore, the concentration for successful phase separation is dependent on the molar mass of the poly(acrylamides) (**Figure S9**).

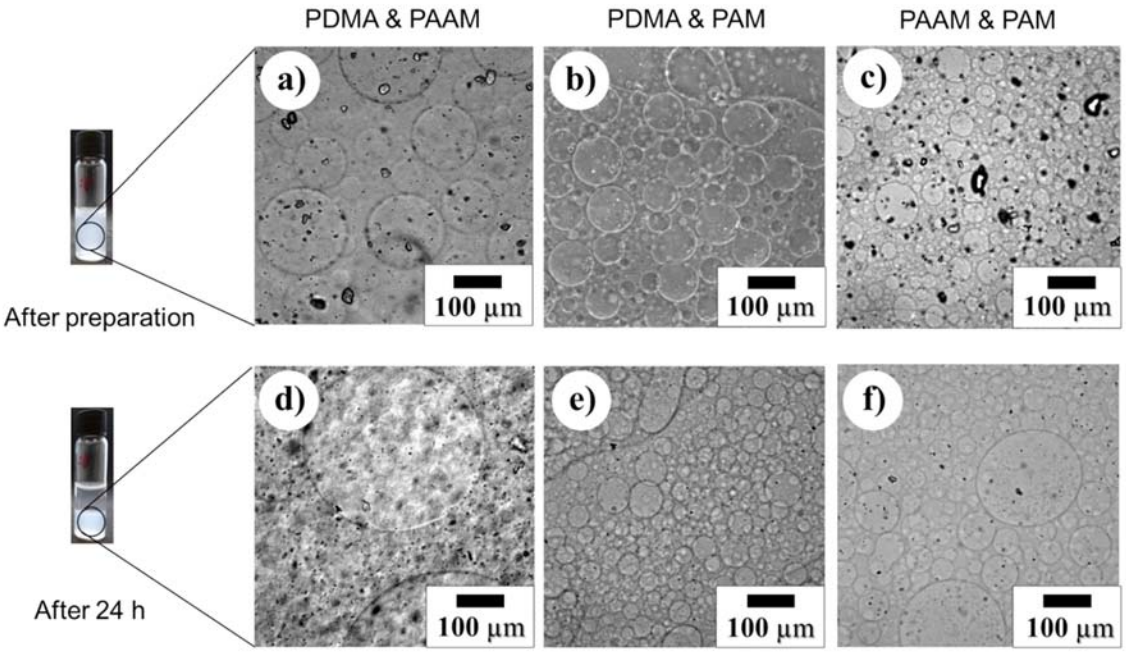

Figure 3. (a-c) Bright field microscopy images of the water in water emulsion of each ATPS (1.5 wt%/1.5 wt%) stabilised with Mg/Al-CO_3-LDH (0.1 wt%) (a) PDMA and PAAM, (b) PDMA and PAM, (c) PAAM and PAM, (d-f) bright field images of the cloudy phase after 24 h and observed phase separation for (d) PDMA and PAAM, (e) PDMA and PAM, (f) PAAM and PAM.

In order to form w/w emulsions, an ATPS for all three polymer combinations (PDMA & PAAM, PDMA & PAM and PAAM & PAM) was prepared at 1.5/1.5 wt%. The concentration was chosen to be placed well in the two-phase region of the phase diagram to obtain a stable ATPS. In order to stabilise the w/w emulsion, a 0.2 wt% aqueous dispersion of Mg/Al-CO_3-LDH nanoparticles[56-58] with 100 nm diameter (**Figure S4**) were added to the ATPS to give a final concentration of 0.1 wt%. Subsequently, the mixture was subjected to ultrasonic treatment for two minutes as well as shaking by hand for one minute. In all three combinations the mixture turned cloudy, which is an

indicator for formation of an emulsion. Next, the emulsions were analysed directly *via* bright field microscopy (**Figure 3 a-c**). After approximately two hours the dispersions started to phase separate, which was completed after around 24 hours. The lower phase remained cloudy for all combinations. Both phases were analysed *via* bright field microscopy to identify the composition of the phases (**Figure 3 d-f** and **Figure S10**). It should be noted that in the bright field images of all combinations aggregated stabiliser particles were visible in the background of the emulsion (black particles). To investigate the stability of the emulsion, the phase separation was analysed *via* bright field microscopy after 4 weeks again (**Figure S11)**. Therefore, the size of the emulsion droplets of all combinations were determined from bright field images and averaged (**Figure S12** and **Table S3**), which revealed slight changes of droplet size with time after phase separation.

Bright field microscopy shows droplet formation for the emulsion based on PDMA and PAAM with an average droplet size around 82 ± 60 µm (**Figure 3a**). For the w/w emulsion of PDMA and PAAM the phase separation begins to start after around two hours and a completely visible phase separation was observed after 24 hours. The upper phase was clear, while the lower phase was cloudy indicating the presence of droplets. In order to confirm the presence or absence of droplets both phases were analysed *via* bright field microscopy after phase separation (**Figure 3d** and **Figure S10a**). In the clear upper phase, the bright field images show no presence of droplets (**Figure S10a**), while the images of the cloudier lower phase show droplets featuring an increased size compared to the emulsion before phase separation. The average droplet size after phase separation, in the cloudy phase was around 122 ± 120 µm. Long-term stability was probed as well, which confirmed that phase separation after four weeks was similar to the phase separation after 24 hours. Also, bright field imaging shows the presence of droplets in the cloudy phase with droplets larger than 100 µm after four weeks (**Figure S11**).

For the system of PDMA and PAM, the bright field measurement displayed the presence of droplets in the w/w emulsion as well (**Figure 3b**). The average droplet size was slightly higher, with around 101 ± 30 µm in comparison to the PDMA and PAAM system. As with all investigated emulsions, phase separation was observed and both phases were analysed *via* bright field microscopy after 24 h (**Figure 3e** and **Figure S10b**). In the images of the clear upper phase, no droplets were visible, while the bright field images of the lower cloudy phase revealed droplets. The average droplet size is around 63 ± 20 µm and smaller in comparison to the emulsion before the phase separation, which might be due to an incomplete phase separation after 24 hours. This reason is supported by the observed droplet size >100 µm after four weeks.

The bright field measurement of the emulsion formed by the ATPS PAAM and PAM, displayed droplets with a size between 30 and 100 µm and an average droplet size of around 64 ± 20 µm (**Figure 3c**), which is the smallest amongst the studied emulsions. After 24 hours and phase separation, droplets between 50 and 200 µm and an average droplet size of around 98 ± 40 µm were observed *via* bright field microscopy in the emulsion phase (**Figure 3f**), while the upper clear phase showed no droplets (**Figure S10c**). After four weeks of phase separation, the emulsion phase displayed droplets in the range of 60 and 150 µm, which is similar to the droplets after 24 hours of phase separation. The high standard deviation is due to the presence of larger and smaller droplets and a broad dispersity in the samples, which was the result of the mixing method (shaking and ultrasonic bath). One way to produce emulsion droplets with lower dispersity is the use of microfluidic devices, for example.

Overall, for all three ATPS combination with Mg/Al-CO_3-LDH as additive, an emulsion could be observed at low concentration (1.5/1.5 wt%). After 24 hours of phase separation, in two of the three combinations the droplet sizes increased significantly. The droplet size increases most likely

due to the phase separation and Ostwald ripening during the phase separation process until an equilibrium is reached. Furthermore, the emulsion was only stable in the lower phase of the ATPS, which is presumably due to the enrichment of LDH particles in the lower phase after phase separation. For the combination of PDAM and PAM the droplet sizes of the emulsion decrease. After four weeks of phase separation, all three combinations display similar droplet sizes >100 µm. Obviously, the prepared w/w emulsions feature a broad dispersity of droplet sizes, which is mainly due to the preparation process. As such, the droplet size and dispersity could mostly likely be tailored via a different preparation method *e.g.* microfluidics or further optimisation in mixing *via* vortex and subsequently ultrasound treatment.

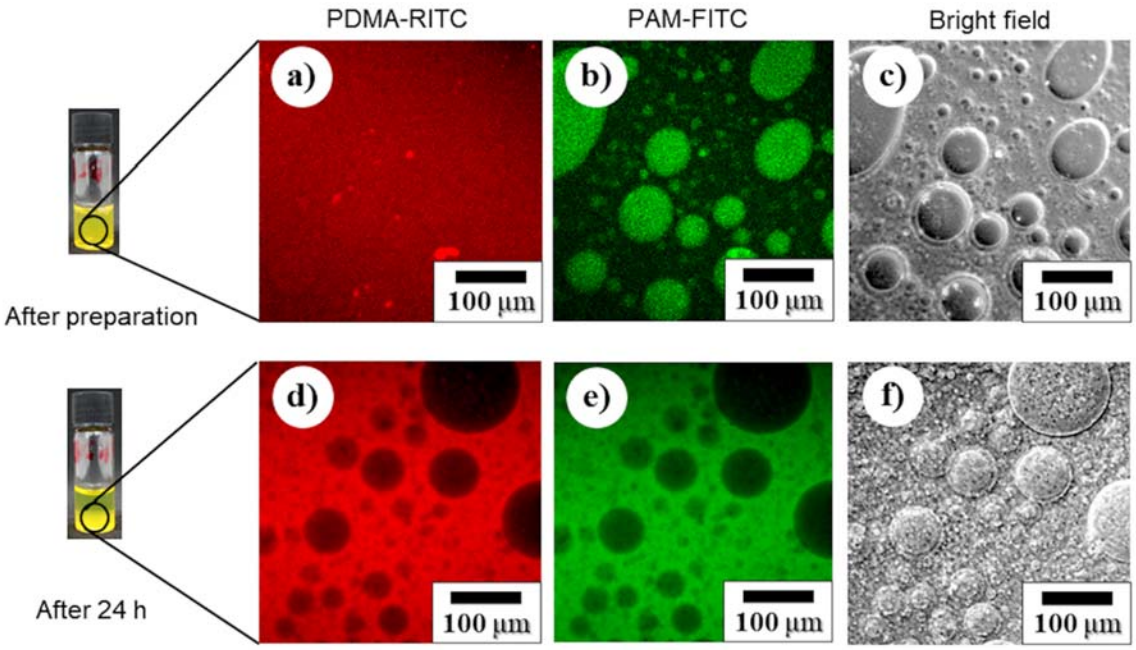

Figure 4. (a-c) CLSM images of the w/w emulsion of PDMA-RITC and PAM-FITC a) PDMA-RITC b) PAM-FITC c) bright field image and (d-f) CLSM images of the lower phase after 24h and observed phase separation d) PDMA-RITC e) PAM-FITC f) bright field image.

In order to localise the polymer type in the emulsion, each polymer type was labelled with a different dye (RITC, FITC and coumarin) and the emulsions were analysed *via* confocal laser scanning microscopy (CLSM) (**Figure 4** and **Figure S13-15**). The emulsions were prepared with a polymer concentration of 1.5/1.5 wt% and stabilised with 0.1 wt% Mg/Al-CO_3-LDH *via* ultrasonic treatment for two minutes as well as shaking by hand for one minute. In the CLSM images for some combinations the stabiliser particles were visible in the background of the emulsion. Especially for the images with coumarin labelled PAAM, due to the similar emission region of LDH particles and coumarin labelled PAAM. For the system PDMA and PAM (**Figure 4 a-f** and **Figure S13**) the CLSM images show that PDMA is located over the entire sample

(**Figure 4a**) and PAM is enriched in the emulsion droplets (**Figure 4b**) for the emulsion direct after preparation. After 24 hours and phase separation each phase was analysed *via* CLSM again. In the upper phase (**Figure S13**) similar to the bright field results, no droplets were visible and both polymers were located over the entire sample. In the CLSM images of the lower phase, droplets were visible and both polymers were located outside the droplets (**Figure 4d-f**). In the system PDMA and PAAM, the CLSM images showed that both polymers were primary locate inside the droplet (**Figure S14a-c**) directly after preparation. After phase separation, no droplets were visible in the upper phase (**Figure S14d-f**) and in the lower phase, both polymers were located outside the observed droplets (**Figure S14g-i**).

The CLSM images of the emulsion formed by the ATPS PAAM and PAM (**Figure S15a-c**), displayed polymer located inside the droplets after preparation. Similar to the other cases, after 24 hours and observation of phase separation, no droplets are visible in the upper phase and the polymers are located over the entire phase (**Figure S15d-f**). The droplet containing lower phase featured both polymers located outside the droplets (**Figure S15g-i**).

Overall, the results show that right after emulsion formation only in the case of PDMA and PAM both polymers are present in different phases (droplet and continuous phase), while for the other cases both polymers are located in the continuous phase. However, after phase separation in all cases the polymers are present in the continuous phases (in the droplet phase). The location of both polymer types in one phase is unexpected as it opposes the situation found for the non-dispersed ATPS. The partitioning of both polymers into the continuous phase is most likely not due to the formation of a coacervate as both polymers tend to demix in the common ATPS system. Thus, we assume that the reason for the uncommon partitioning lies in the emulsion formation itself, *i.e.* the addition of stabiliser and dispersion of the phases. One reason is the change of the polymer ratio

after phase separation. An experiment with the polymer ratio PDMA/PAM of 1:4 that corresponds to the equilibrium concentration after 24h phase separation shows a similar partitioning of both polymers directly after preparation without equilibration (**Figure S16**). The dye functionalization does not have not an influence on the phase behaviour of the polymers in the emulsion. The partitioning of both polymers is the same with only one dye present at the time (**Figure S17**).

Clearly, the stabiliser has a profound effect on the aggregative polymer phase behavior. Thus, the effect of stabiliser amount was probed. At low stabiliser concentration (0.05 wt%) the polymers are present inside the droplet but still aggregative phase separation is observed. At higher stabiliser concentration (0.5 wt%) both polymers are a present in the continuous phase (**Figure S18**) as observed at 0.1 wt%. Consequently, we conclude that aggregation takes place regardless of particle concentration but the particle concentration significantly influences the location of polymer aggregates. The large number of hydroxyl groups on the LDH nanoparticles could influence the polymer separation and led to aggregation. To confirm aggregation of the utilized polymers via LDH nanoparticles, DLS measurements were performed. DLS measurements of the LDH nanoparticles in combination with the polymer in aqueous solution showed the formation of large aggregates with sizes above 1 μm (**Figure S19** and **Table S4**), which indicates an interaction between polymers and nanoparticles. Such an aggregate formation was described in the formation of nanocomposites from LDH nanoparticles and polymers for various polymers *e.g.* polyacrylamide[59-61] or double hydrophilic block copolymers.[62] As such, we assume that the aggregative phase separation behavior is due to the aggregation between the polymers and LDH nanoparticles.

The feature of our ultra-high molar mass polyacrylamide w/w emulsions system is relevant for application, as water droplets and polymer-enriched phases are formed, similar to what we found

in previous studies with double hydrophilic block copolymers.[47, 63] That effect might be useful for partitioning and separation of biomolecules.

A3PS of ultra-high molar mass poly(acrylamides)

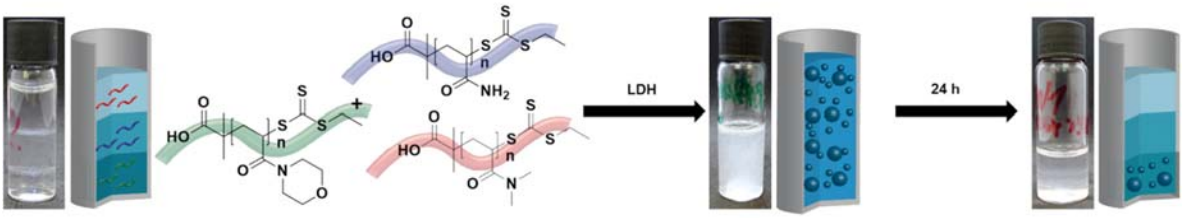

Scheme 2. Schematics of the water-in-water emulsion of the A3PS (PAAM, PAM and PDMA) stabilised by Mg/Al-LDH nanoparticles.

In order to test the limitations of the system, an aqueous three phase system (A3PS) of the three poly(acrylamides) was investigated. Therefore, polymer solutions with different concentrations were prepared *e.g.* 6 wt% total polymer concentration (2 wt% PDMA/2 wt% PAAM/2 wt% PAM). The solution was mixed, equilibrated at ambient temperature to demix, investigated and diluted. Upon dilution the A3PS turned into an ATPS and finally into an one phase system. In order to receive an in-depth look into the A3PS, the phase diagram was prepared. The phase diagram (**Figure 5a** and **S20**) shows two phase transitions, one for the three phase/two phase border and one for the two phase/one phase border. The three phase/two phase border for the equal starting concentration of all polymers (2/2/2) was observed around a total polymer concentration of 2.1 wt% (0.7 wt% PDMA/ 0.7 wt% PAAM/ 0.7 wt% PAM) and the two phase/one phase border around a total polymer concentration of 1.5 wt% (0.5/0.5/0.5). The presence of the polymers in the individual phases were detected *via* ^{1}H-NMR in D_2O with DMF as internal standard after the phase

separation (**Figure S21**) and the polymer concentration detected (**Figure S22**). The ^{1}H-NMR data showed that every phase of the three phases was enriched with one polymer. However, the small amounts of the other polymers were present in every phase as well, which was also expressed via partition coefficients (Table S4).

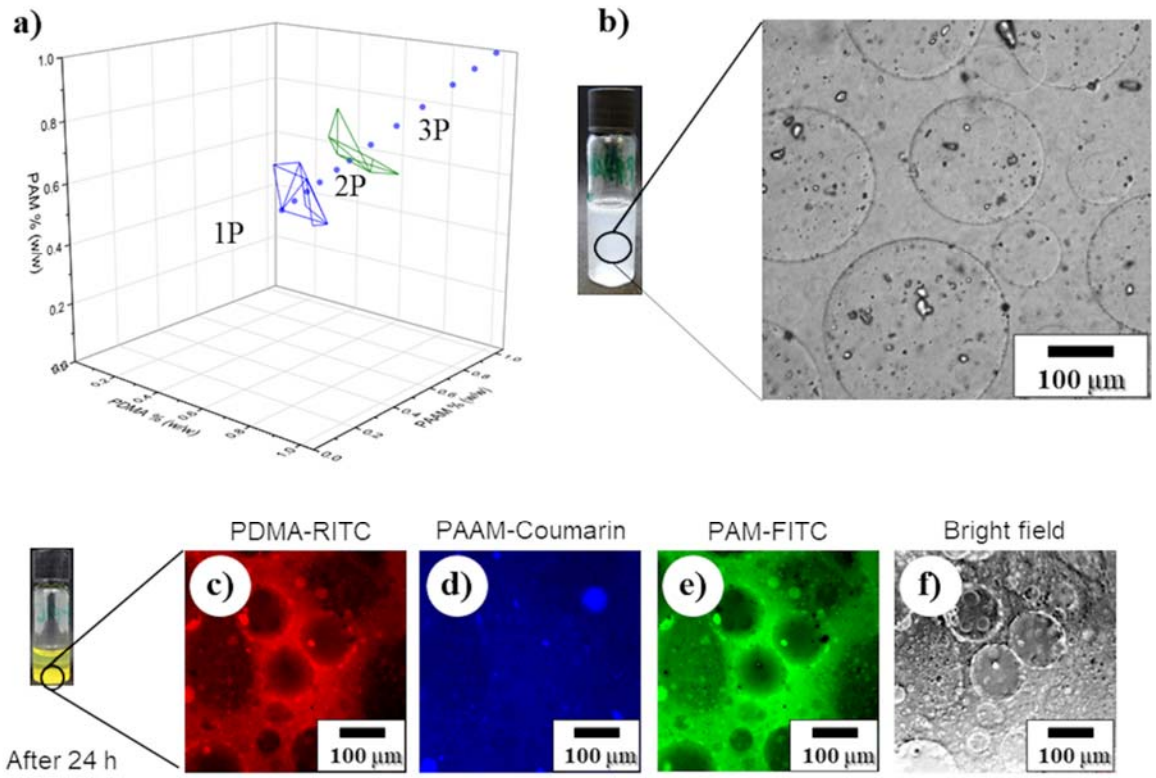

Figure 5. (a) Phase diagram of the A3PS of PDMA, PAAM and PAM with one-phase/two-phase (1P/2P) border (blue line) and two-phase/three-phase (2P/3P) border (green line), (b) Bright field image of the w/w emulsion of A3PS with Mg/Al-LDH, (c-f) CLSM images of the w/w emulsion of A3PS after 24 hours and phase separation (c) PDMA-RITC, (d) Coumarin-PAAM, (e) PAM-FITC and (f) bright field.

Additionally, a w/w emulsion was prepared with the A3PS and Mg/Al-CO_3-LDH as additive. In comparison to the w/w emulsion formed by the different ATPSs the total polymer concentration was set to 3 wt% (1/1/1) and the LDH concentration 0.1 wt%. The w/w emulsion was analysed *via* bright field microscopy (**Figure 5b**) revealing droplets with a diameter between 50 and 250 µm with an average particle size around 184 ± 70 µm indicating a successful w/w emulsion. In order to locate the polymers in the emulsion, the labelled polymers were added in the preparation of the emulsion and the emulsion was analysed *via* CLSM before and after phase separation after 24 h. Similar to the two polymer systems, the CLSM images of the mixture showed water droplets in a polymer-enriched matrix (**Figure S23**). After phase separation (24 h) the upper and the middle phase of the A3PS did not display droplets (**Figure S23**). In contrast, the lower phase contained droplets, where the polymers are located outside of the emulsion droplet (**Figure 5c-f**).

Overall, the aqueous solution of the three polyacrylamides, leads to A3PS. Upon dilution the A3PS turns into an ATPS around a total polymer concentration of 2.1 wt% and into an one phase system around a total polymer concentration of 1.5 wt%. Furthermore, the A3PS can form, stabilised by LDH particles, a w/w emulsion before and after phase separation as well. Similar to the two-polymer system, the polymers are located outside the emulsion droplets in the lower phase. After phase separation the emulsion was again only stable in the lower phase presumably, due to the enrichment of LDH particles in the lower phase.

Conclusion

The three ultra-high molar mass polyacrylamides PDMA, PAAM and PAM were synthesised *via* photo induced RAFT polymerisation and were subjected to ATPS formation. In addition, the ATPSs were used to form w/w emulsions, stabilised with Mg/Al-CO_3-LDH nanoparticles. The

emulsion was stable in the mixture and after phase separation, in the lower phase, for at least four weeks. The polymers were located in the emulsion via CLSM, showing that at first polymer-containing droplets in water were formed directly after dispersion and water droplets in polymer matrix after phase separation. Furthermore, the solution of all three polymers in water, revealed the formation of an A3PS, which is stable at low concentration as well. The emulsion formed by the A3PS was indicated as water in polymer droplets for the emulsion before and after phase separation. Interestingly, in most cases polymers were enriched in the same phase, which has several implications for future applications. The enrichment of polymers and the requirement of low polymer concentrations might be useful for bio molecule separation or the compartmentalisation of aqueous environments in catalysis in the future.

ASSOCIATED CONTENT

Supporting Information. Experimental procedures and analytical data on the utilised polymers and LDH particles; analytical data on the multi-phase systems and polymer partitioning; analytical data on the w/w emulsions.

AUTHOR INFORMATION

Corresponding Author

*Dr. B. V. K. J. Schmidt

School of Chemistry, University of Glasgow, Glasgow G12 8QQ, UK

Email: bernhard.schmidt@glasgow.ac.uk

Present Addresses

Dr. M. Pavlovic

BioSense Institute, University of Novi Sad, Dr Zorana Djindjica 1, III-8, 21000 Novi Sad, Serbia

Author Contributions

The manuscript was written through contributions of all authors. All authors have given approval to the final version of the manuscript.

Funding Sources

University of Glasgow

German Research Foundation (grant no. SCHM 3282/3-1)

Swiss National Science Foundation (project no. P2GEP2_181528)

Max Planck Society

ACKNOWLEDGMENT

The authors acknowledge Marlies Gräwert, June Southgathe and Sascha Prentzel for SEC measurements. B.S. and A.P. acknowledge funding from the University of Glasgow and the German Research Foundation (grant no. SCHM 3282/3-1). M.P. acknowledges financial support from the Swiss National Science Foundation with the project number P2GEP2_181528 and the Max Planck Society.

REFERENCES

1. Roy, I.; Gupta, M. N. Smart polymeric materials: emerging biochemical applications. *Chem. Biol.* **2003,** 10 (12), 1161-1171.

2. Haag, R.; Kratz, F. Polymer therapeutics: concepts and applications. *Angew. Chem., Int. Ed.* **2006,** 45 (8), 1198-1215.
3. Rhim, J.-W.; Park, H.-M.; Ha, C.-S. Bio-nanocomposites for food packaging applications. *Prog. Polym. Sci.* **2013,** 38 (10-11), 1629-1652.
4. Pereira, J. F.; Freire, M. G.; Coutinho, J. A. Aqueous two-phase systems: Towards novel and more disruptive applications. *Fluid Phase Equilib.* **2020,** 505, 112341.
5. Albertsson, P. Fractionation of particles and macromolecules in aqueous two-phase systems. *Biochem. Pharmacol.* **1961,** 5 (4), 351-358.
6. Hatti-Kaul, R. Aqueous two-phase systems. *Mol. Biotechnol.* **2001,** 19 (3), 269-277.
7. Grilo, A. L.; Raquel Aires-Barros, M.; Azevedo, A. M. Partitioning in aqueous two-phase systems: fundamentals, applications and trends. *Sep. Purif. Rev.* **2016,** 45 (1), 68-80.
8. Chao, Y.; Shum, H. C. Emerging aqueous two-phase systems: from fundamentals of interfaces to biomedical applications. *Chem. Soc. Rev.* **2020,** 49 (1), 114-142.
9. Rito-Palomares, M.; Negrete, A.; Galindo, E.; Serrano-Carreon, L. Aroma compounds recovery from mycelial cultures in aqueous two-phase processes. *J. Chromatogr. B: Biomed. Sci. Appl.* **2000,** 743 (1-2), 403-408.
10. Keating, C. D. Aqueous phase separation as a possible route to compartmentalization of biological molecules. *Acc. Chem. Res.* **2012,** 45 (12), 2114-2124.
11. Benavides, J.; Aguilar, O.; Lapizco-Encinas, B. H.; Rito-Palomares, M. Extraction and purification of bioproducts and nanoparticles using aqueous two-phase systems strategies. *Chem. Eng. Technol.* **2008,** 31 (6), 838-845.
12. Asenjo, J. A.; Andrews, B. A. Aqueous two-phase systems for protein separation: a perspective. *J. Chromatogr. A* **2011,** 1218 (49), 8826-8835.
13. Rodrigues, G. D.; da Silva, M. d. C. H.; da Silva, L. H. M.; Paggioli, F. J.; Minim, L. A.; dos Reis Coimbra, J. S. Liquid–liquid extraction of metal ions without use of organic solvent. *Sep. Purif. Technol.* **2008,** 62 (3), 687-693.
14. da Rocha Patrício, P.; Mesquita, M. C.; da Silva, L. H. M.; da Silva, M. C. H. Application of aqueous two-phase systems for the development of a new method of cobalt (II), iron (III) and nickel (II) extraction: a green chemistry approach. *J. Hazard. Mater.* **2011,** 193, 311-318.
15. Ryden, J.; Albertsson, P.-a. Interfacial tension of dextran—polyethylene glycol—water two—phase systems. *J. Colloid Interface Sci.* **1971,** 37 (1), 219-222.
16. Yuan, H.; Ma, Q.; Song, Y.; Tang, M. Y.; Chan, Y. K.; Shum, H. C. Phase-Separation-Induced Formation of Janus Droplets Based on Aqueous Two-Phase Systems. *Macromol. Chem. Phys.* **2017,** 218 (2), 1600422.
17. Pavlovic, M.; Antonietti, M.; Schmidt, B. V. K. J.; Zeininger, L. Responsive Janus and Cerberus emulsions via temperature-induced phase separation in aqueous polymer mixtures. *J. Colloid Interface Sci.* **2020,** 575, 88-95.
18. Dominak, L. M.; Gundermann, E. L.; Keating, C. D. Microcompartmentation in artificial cells: pH-induced conformational changes alter protein localization. *Langmuir* **2010,** 26 (8), 5697-5705.
19. Pavlovic, M.; Plucinski, A.; Zhang, J.; Antonietti, M.; Zeininger, L.; Schmidt, B. V. K. J. Cascade kinetics in an enzyme-loaded aqueous two-phase system. *Langmuir* **2020,** 36 (6), 1401-1408.
20. Esquena, J. Water-in-water (W/W) emulsions. *Curr. Opin. Colloid Interface Sci.* **2016,** 25, 109-119.

21. Nicolai, T.; Murray, B. Particle stabilized water in water emulsions. *Food Hydrocolloids* **2017,** 68, 157-163.
22. Grinberg, V. Y.; Tolstoguzov, V. Thermodynamic incompatibility of proteins and polysaccharides in solutions. *Food Hydrocolloids* **1997,** 11 (2), 145-158.
23. Buzza, D. M. A.; Fletcher, P. D.; Georgiou, T. K.; Ghasdian, N. Water-in-Water Emulsions Based on Incompatible Polymers and Stabilized by Triblock Copolymers–Templated Polymersomes. *Langmuir* **2013,** 29 (48), 14804-14814.
24. Poortinga, A. T. Microcapsules from Self-Assembled Colloidal Particles Using Aqueous Phase-Separated Polymer Solutions. *Langmuir* **2008,** 24 (5), 1644-1647.
25. Vis, M.; Opdam, J.; Van't Oor, I. S.; Soligno, G.; Van Roij, R.; Tromp, R. H.; Erné, B. H. Water-in-water emulsions stabilized by nanoplates. *ACS Macro Lett.* **2015,** 4 (9), 965-968.
26. Kim, J. W.; Lee, D.; Shum, H. C.; Weitz, D. A. Colloid surfactants for emulsion stabilization. *Adv. Mater.* **2008,** 20 (17), 3239-3243.
27. Forciniti, D.; Hall, C.; Kula, M. Interfacial tension of polyethyleneglycol-dextran-water systems: influence of temperature and polymer molecular weight. *J. Biotechnol.* **1990,** 16 (3-4), 279-296.
28. Scholten, E.; Visser, J. E.; Sagis, L. M.; van der Linden, E. Ultralow interfacial tensions in an aqueous phase-separated gelatin/dextran and gelatin/gum arabic system: A comparison. *Langmuir* **2004,** 20 (6), 2292-2297.
29. Peddireddy, K. R.; Nicolai, T.; Benyahia, L.; Capron, I. Stabilization of water-in-water emulsions by nanorods. *ACS Macro Lett.* **2016,** 5 (3), 283-286.
30. Zhang, J.; Hwang, J.; Antonietti, M.; Schmidt, B. V. K. J. Water-in-water pickering emulsion stabilized by polydopamine particles and cross-linking. *Biomacromolecules* **2018,** 20 (1), 204-211.
31. Zhang, J.; Kumru, B.; Schmidt, B. V. K. J. Supramolecular Compartmentalized Hydrogels via Polydopamine Particle-Stabilized Water-in-Water Emulsions. *Langmuir* **2019,** 35 (34), 11141-11149.
32. Pavlovic, M.; Plucinski, A.; Zeininger, L.; Schmidt, B. V. K. J. Temperature sensitive water-in-water emulsions. *Chem. Commun.* **2020,** 56 (50), 6814-6817.
33. Hu, Z.; Chen, G. Novel nanocomposite hydrogels consisting of layered double hydroxide with ultrahigh tensibility and hierarchical porous structure at low inorganic content. *Adv. Mater.* **2014,** 26 (34), 5950-5956.
34. Pavlovic, M.; Rouster, P.; Bourgeat-Lami, E.; Prevot, V.; Szilagyi, I. Design of latex-layered double hydroxide composites by tuning the aggregation in suspensions. *Soft Matter* **2017,** 13 (4), 842-851.
35. Inam, M.; Jones, J. R.; Pérez-Madrigal, M. M.; Arno, M. C.; Dove, A. P.; O'Reilly, R. K. Controlling the size of two-dimensional polymer platelets for water-in-water emulsifiers. *ACS Cent. Sci.* **2018,** 4 (1), 63-70.
36. Mace, C. R.; Akbulut, O.; Kumar, A. A.; Shapiro, N. D.; Derda, R.; Patton, M. R.; Whitesides, G. M. Aqueous multiphase systems of polymers and surfactants provide self-assembling step-gradients in density. *J. Am. Chem. Soc.* **2012,** 134 (22), 9094-9097.
37. Akbulut, O.; Mace, C. R.; Martinez, R. V.; Kumar, A. A.; Nie, Z.; Patton, M. R.; Whitesides, G. M. Separation of nanoparticles in aqueous multiphase systems through centrifugation. *Nano Lett.* **2012,** 12 (8), 4060-4064.
38. Song, Y.; Sauret, A.; Cheung Shum, H. All-aqueous multiphase microfluidics. *Biomicrofluidics* **2013,** 7 (6), 061301.

39. Sauret, A.; Cheung Shum, H. Forced generation of simple and double emulsions in all-aqueous systems. *Appl. Phys. Lett.* **2012,** 100 (15), 154106.
40. Beldengrün, Y.; Dallaris, V.; Jaén, C.; Protat, R.; Miras, J.; Calvo, M.; Garcia-Celma, M. J.; Esquena, J. Formation and stabilization of multiple water-in-water-in-water (W/W/W) emulsions. *Food Hydrocolloids* **2020,** 102, 105588.
41. Diamond, A. D.; Hsu, J. T. Fundamental studies of biomolecule partitioning in aqueous two-phase systems. *Biotechnol. Bioeng.* **1989,** 34 (7), 1000-1014.
42. Forciniti, D.; Hall, C.; Kula, M.-R. Influence of polymer molecular weight and temperature on phase composition in aqueous two-phase systems. *Fluid Phase Equilib.* **1991,** 61 (3), 243-262.
43. Tubío, G.; Pellegrini, L.; Nerli, B. B.; Picó, G. A. Liquid− liquid equilibria of aqueous two-phase systems containing poly (ethylene glycols) of different molecular weight and sodium citrate. *J. Chem. Eng. Data* **2006,** 51 (1), 209-212.
44. Saravanan, S.; Rao, J. R.; Nair, B. U.; Ramasami, T. Aqueous two-phase poly (ethylene glycol)–poly (acrylic acid) system for protein partitioning: Influence of molecular weight, pH and temperature. *Process Biochem.* **2008,** 43 (9), 905-911.
45. Schmidt, B. V. K. J. Double Hydrophilic Block Copolymer Self-Assembly in Aqueous Solution. *Macromol. Chem. Phys.* **2018,** 219 (7), 1700494.
46. Willersinn, J.; Bogomolova, A.; Cabré, M. B.; Schmidt, B. V. K. J. Vesicles of double hydrophilic pullulan and poly (acrylamide) block copolymers: A combination of synthetic-and bio-derived blocks. *Polym. Chem.* **2017,** 8 (7), 1244-1254.
47. Plucinski, A.; Willersinn, J.; Lira, R. B.; Dimova, R.; Schmidt, B. V. K. J. Aggregation and Crosslinking of Poly (N, N-dimethylacrylamide)-b-pullulan Double Hydrophilic Block Copolymers. *Macromol. Chem. Phys.* **2020,** 221 (13), 2000053.
48. Xu, J.; Jung, K.; Atme, A.; Shanmugam, S.; Boyer, C. A robust and versatile photoinduced living polymerization of conjugated and unconjugated monomers and its oxygen tolerance. *J. Am. Chem. Soc.* **2014,** 136 (14), 5508-5519.
49. Read, E.; Guinaudeau, A.; Wilson, D. J.; Cadix, A.; Violleau, F.; Destarac, M. Low temperature RAFT/MADIX gel polymerisation: access to controlled ultra-high molar mass polyacrylamides. *Polym. Chem.* **2014,** 5 (7), 2202-2207.
50. Carmean, R. N.; Becker, T. E.; Sims, M. B.; Sumerlin, B. S. Ultra-high molecular weights via aqueous reversible-deactivation radical polymerization. *Chem* **2017,** 2 (1), 93-101.
51. An, Z. 100th anniversary of macromolecular science viewpoint: achieving ultrahigh molecular weights with reversible deactivation radical polymerization. *ACS Macro Lett.* **2020,** 9 (3), 350-357.
52. Carmean, R. N.; Sims, M. B.; Figg, C. A.; Hurst, P. J.; Patterson, J. P.; Sumerlin, B. S. Ultrahigh molecular weight hydrophobic acrylic and styrenic polymers through organic-phase photoiniferter-mediated polymerization. *ACS Macro Lett.* **2020,** 9 (4), 613-618.
53. Allison-Logan, S.; Karimi, F.; Sun, Y.; McKenzie, T. G.; Nothling, M. D.; Bryant, G.; Qiao, G. G. Highly living stars via core-first photo-RAFT polymerization: exploitation for ultra-high molecular weight star synthesis. *ACS Macro Lett.* **2019,** 8 (10), 1291-1295.
54. Schmidt, B. V. K. J.; Hetzer, M.; Ritter, H.; Barner-Kowollik, C. Cyclodextrin-complexed RAFT agents for the ambient temperature aqueous living/controlled radical polymerization of acrylamido monomers. *Macromolecules* **2011,** 44 (18), 7220-7232.
55. Skey, J.; O'Reilly, R. K. Facile one pot synthesis of a range of reversible addition–fragmentation chain transfer (RAFT) agents. *Chem. Commun.* **2008,** (35), 4183-4185.

56. Pavlovic, M.; Huber, R.; Adok-Sipiczki, M.; Nardin, C.; Szilagyi, I. Ion specific effects on the stability of layered double hydroxide colloids. *Soft Matter* **2016,** 12 (17), 4024-4033.
57. Mishra, G.; Dash, B.; Pandey, S. Layered double hydroxides: A brief review from fundamentals to application as evolving biomaterials. *Appl. Clay Sci.* **2018,** 153, 172-186.
58. Xu, Z. P.; Stevenson, G.; Lu, C.-Q.; Lu, G. Q. Dispersion and size control of layered double hydroxide nanoparticles in aqueous solutions. *J. Phys. Chem. B* **2006,** 110 (34), 16923-16929.
59. Hu, Z.; Chen, G. Aqueous dispersions of layered double hydroxide/polyacrylamide nanocomposites: preparation and rheology. *J. Mater. Chem. A* **2014,** 2 (33), 13593-13601.
60. Yang, X.-J.; Zhang, P.; Li, P.; Li, Z.; Xia, W.; Zhang, H.; Di, Z.; Wang, M.; Zhang, H.; Niu, Q. J. Layered double hydroxide/polyacrylamide nanocomposite hydrogels: Green preparation, rheology and application in methyl orange removal from aqueous solution. *J. Mol. Liq.* **2019,** 280, 128-134.
61. Fu, P.; Xu, K.; Song, H.; Chen, G.; Yang, J.; Niu, Y. Preparation, stability and rheology of polyacrylamide/pristine layered double hydroxide nanocomposites. *J. Mater. Chem.* **2010,** 20 (19), 3869-3876.
62. Layrac, G.; Harrisson, S.; Destarac, M.; Gerardin, C.; Tichit, D. Comprehensive study of the formation of stable colloids of CuAl layered double hydroxide assisted by double hydrophilic block copolymers. *Applied Clay Science* **2020,** 193, 105673.
63. Lira, R. B.; Willersinn, J.; Schmidt, B. V. K. J.; Dimova, R. Selective Partitioning of (Biomacro) molecules in the Crowded Environment of Double-Hydrophilic Block Copolymers. *Macromolecules* **2020,** 53 (22), 10179-10188.